Unclassified
SECURITY CLASSIFICATION OF THIS PAGE

AIR FILE COPY

REPORT DOCUMENTATION PAGE

AD-A208 438

1b. RESTRICTIVE MARKINGS	
2b. DECLASSIFICATION / DOWNGRADING SCHEDULE	3. DISTRIBUTION / AVAILABILITY OF REPORT: Approved for public release distribution unlimited.
4. PERFORMING ORGANIZATION REPORT NUMBER(S)	5. MONITORING ORGANIZATION REPORT NUMBER(S)
6a. NAME OF PERFORMING ORGANIZATION: Rensselaer Polytechnic Inst. / 6b. OFFICE SYMBOL (If applicable)	7a. NAME OF MONITORING ORGANIZATION: ONR
6c. ADDRESS (City, State, and ZIP Code): Dept. of Chemistry, Troy, NY 12180-3590	7b. ADDRESS (City, State, and ZIP Code): Department of Navy, Arlington, VA 22217
8a. NAME OF FUNDING / SPONSORING ORGANIZATION: ONR / 8b. OFFICE SYMBOL (If applicable)	9. PROCUREMENT INSTRUMENT IDENTIFICATION NUMBER
8c. ADDRESS (City, State, and ZIP Code): Department of Navy, Arlington, VA 22217	10. SOURCE OF FUNDING NUMBERS: PROGRAM ELEMENT NO. N0014-85-K 0632 / PROJECT NO. / TASK NO 625-856 / WORK UNIT ACCESSION NO

11. TITLE (Include Security Classification): TECH. REP. #9
RESIST SENSITIVITY ENHANCEMENT BY RADIATION-INDUCED MODIFICATION-UNCLAIMED

12. PERSONAL AUTHOR(S): J.A. Moore, J.-O Choi, S.-Y. Kim, J.C. Corelli

13a. TYPE OF REPORT	13b. TIME COVERED FROM ____ TO ____	14. DATE OF REPORT (Year, Month, Day)	15. PAGE COUNT
Publication		June, 1989	

16. SUPPLEMENTARY NOTATION: PROC. 172nd MEETING OF THE ELECTROCHEM. SOC., MARCH, 1988

17. COSATI CODES			18. SUBJECT TERMS (Continue on reverse if necessary and identify by block number)
FIELD	GROUP	SUB-GROUP	

19. ABSTRACT (Continue on reverse if necessary and identify by block number)

89 6 02 112

20. DISTRIBUTION / AVAILABILITY OF ABSTRACT: ☒ UNCLASSIFIED/UNLIMITED ☐ SAME AS RPT. ☐ DTIC USERS	21. ABSTRACT SECURITY CLASSIFICATION: Unclassified
22a. NAME OF RESPONSIBLE INDIVIDUAL: Kenneth J. Wynne	22b. TELEPHONE (Include Area Code): (202) 696-4410 / 22c. OFFICE SYMBOL

DD FORM 1473, 84 MAR — 83 APR edition may be used until exhausted. All other editions are obsolete.

SECURITY CLASSIFICATION OF THIS PAGE
Unclassified

Office of Naval Research
Contract N0014-85-K-0632
R & T Code 413c014

Technical Report No. 9

"Resist Sensitivity Enhancement by Radiation-induced Modification"

by

J. A. Moore, Jin-O Choi, Sang-Youl Kim, John C. Corelli

Published in

Proceedings of the 172nd Meeting of the Electrochemical Society,
March, 1988

Department of Chemistry
Rensselaer Polytechnic Institute
Troy, New York 12180-3590

June, 1989

RESIST SENSITIVITY ENHANCEMENT BY RADIATION-INDUCED MODIFICATION

J. A. Moore*, J. O. Choi*, S. Y. Kim* and J. C. Corelli†
Department of Chemistry*
and
Center for Integrated Electronics†
Rensselaer Polytechnic Institute
Troy, NY 12180-3590

ABSTRACT

Exposure of poly(methylmethacrylate), PMMA, to electrons, protons, x-rays and ultraviolet radiation creates free radicals which combine with acrylic acid in a chain reaction to form graft and/or block copolymers with solubilities different from PMMA. Appropriate solvents develop negative images generated at doses on the order of 1,000 times less than those needed to form positive images in PMMA. At doses exceeding optimum values growth of the image occurs vertically and laterally. High fidelity replication can be accomplished by controlling dose and by using more aggressive solvents. Enhanced dry etch resistance can be conferred on the acrylic acid-modified PMMA by permitting it to imbibe calcium ion. An image is developed by exposure to an oxygen plasma which consumes unmodified PMMA and generates calcium oxide in the modified regions. The calcinated images are resistant to a fluorine plasma which etches exposed silicon dioxide transferring the modified image into the oxide layer. The modified polymer residue can be stripped using Caro's acid. Replacing acrylic acid with chloroacrylic acid permits the use of Auger spectroscopy and SIMS to indicate that the modifying monomer penetrates the entire thickness of the film. Residual solvent enhances the amount of modification in UV exposures.

INTRODUCTION

In 1981, shortly after the Center for Integrated Electronics was established at RPI, we began a program to study, by chemical means, the transformations engendered in polymeric materials by a variety of radiation types. The following paper is an account of our work in this area and I have not made an attempt to present similar efforts by other research groups. We chose poly(methylmethacrylate), PMMA, as the polymer to study because of its widespread use in microlithography.[1,2] One of the first approaches we used was to expose a silicon wafer coated with PMMA to an electron beam and subsequently to dimethyldichlorosilane. If, as the literature suggests[3], the radiation damaged regions of the film are more permeable to solvent, dimethyldichlorosilane should enter them and be trapped. Evaporation of reagent adsorbed to non-irradiated regions followed by treatment with water generates an interpenetrating network of poly(dimethylsiloxane) dispersed in PMMA which can be imaged by etching in an oxygen plasma. (Fig. 1). The net effect is a reversal of image polarity from positive to negative for PMMA.[4] Fig. 2 is an electron micrograph of a rather sharply delineated 2μ line generated in this fashion. Encouraged by this initial success we sought a monomer which could be introduced into the film and which would <u>chemically</u> bond to, and modify the solubility properties of, the irradiated regions. Wayne Moreau of IBM made us aware of the work of Cazard et al.[5] who showed that acrylic acid could be chemically bonded to PMMA after exposure to an electron beam at a dose of 10^{-8} C/cm^2. We decided to repeat their work with electrons and to determine if this approach was general with respect to the type of radiation used.

RESULTS AND DISCUSSION

In Fig. 3 is shown a comparison of standard PMMA lithography and what we call "in situ modification". The basic difference is that we make use of the reactive centers to initiate a chain reaction in which <u>many</u> molecules of the modifying monomer are attached to PMMA for <u>each</u> chain cleavage event. Thus, a high level of solubility alteration can be attained for a relatively small radiation dose. An examination of the electron spin resonance properties of

the radiation damaged films revealed that the same free radical species is generated irrespective of the type of radiation used.[6] A schematic of the generation of free radical sites in PMMA upon irradiation is shown in Fig. 4.[7] It should be noted that the reaction pathways shown are not, in principle, restricted to being generated by one particular sort of radiation. In terms of application to lithography, Fig. 5 shows how this process of radiation-induced modification is used to generate negative images. It can be seen that in-situ modification adds only one step (the introduction of the modifying monomer) to the conventional steps of spin-coating, irradiation and development. The relatively simple apparatus which is used is shown in Fig. 6 and consists of an evacuable chamber in which the irradiated polymer film is exposed to the vapor above a degassed solution of freshly distilled acrylic acid in water(10%). The individual steps used in the basic process are outlined in Fig. 7 and include irradiation, exposure to monomer (after evacuation of the chamber to a base pressure of 10^{-6} torr) at 60°C for 10-40 min., baking at 120°C for 15 min. and development using a selected solvent at 40°C for 5-10 min.

After irradiation with an electron beam at a nominal dose of 10^{-8} C/cm^2 (a sensitivity enhancement of 1,000 X) and exposure to monomer, but before development, the selective permeation of the exposed areas is readily apparent to the naked eye, as shown in Fig. 8. Clearly modification of the PMMA film is restricted mainly to the areas which have undergone radiation damage.[8] After development with toluene, well defined images can be obtained as shown for the 2μ line in the electron micrograph in Fig. 9.

Similar results were obtained using X-rays.[9] When PMMA is irradiated with X-rays generated at the National Synchrotron Light Source at Brookhaven National Laboratory at a dose of 1 J/cm^2 through an X-ray mask generously supplied by IBM the positive image shown in Fig. 10 is obtained after development. Using the same mask for the in situ process we obtain the clearly defined negative images shown in Fig.11. The remarkable difference between these two micrographs is that the second structure was formed by a dose of 1 mJ/cm^2, a 1,000-fold enhancement of sensitivity. Image fidelity of the positive and negative tone processes is examined in Fig. 12, where it may be seen that they compare favorably in this regard.

The gracious assistance of John Randall at MIT's Lincoln Laboratory gave us access to a proton beam with which the results shown in Fig.13 - 16 were obtained.[10] The sensitivity factor of 1000 is once again apparent in the comparison given in Fig.13. As was the case with X-ray exposures, the fidelity of image replication is seen to be quite good, despite the disparity in doses. One of the attractive features of ion beam exposures is the small structures which can be generated, as demonstrated in Fig.15 where an approximately 0.25μ line is shown. A further indication that the modifying monomer penetrates into the bulk of the resist was obtained serendipitously by overdeveloping a wafer which had been exposed to a proton beam, Fig.16. The "mushroom cap" feature represents that region in which the incident ions dissipated their energy (the damage track), while the darker, "stem portion" is PMMA which remains unmodified because it was untouched by the impinging particles. Clearly, modification only occurs in the radiation-damaged portions of the resist.

Similar results are obtained with deep ultraviolet radiation (DUV) as shown in Fig. 17. Here a direct comparison is made between a positive tone image generated at 1 J/cm^2 and a negative tone image generated by the in situ process at a dose of 6 mJ/cm^2, a sensitivity enhancement of almost 1,000. The utility of this approach to UV generation of submicron images is seen in Fig. 18, where a 0.75 μ line was formed at approximately the same dose as the previous figure.

A comparison of the enhancements obtained for all four radiation types is collected in Fig. 19. The "normal" dose for positive tone is included for comparison and the positive tone dose data are given in terms of incident energy and particle flux. It is apparent that, based on either view, the proton beam gives rise to the highest extent of modification. This observation presumably reflects the fact that the impact of the more massive proton causes more bond ruptures in the resist resulting in the incorporation of more modifying monomer.

A comparison of the weight gained by a UV-irradiated film of PMMA upon exposure to acrylic acid vapor versus time for several doses is given in Fig. 20. It may be seen that the higher the dose is, the more monomer is incorporated for a particular reaction temperature. Related data for this sysytem is presented in Fig. 21 where it may be seen that for a given dose and reaction time, the

weight gain is greater at a higher reaction temperature. When we attempted to follow dissolution rate as a function of dose using a laser interferometer we were frustrated because the refractive index of PMMA matches those of the solvents we wanted to use. Therefore, we were forced to make the necessary measurements using a Dektak profilometer. It soon became apparent that, particularly at the higher doses, the generated image was "growing" above the surface of the resist. This phenomenon of "overgrowth", i.e. generation of polymer above the surface of the original resist thickness, is apparently not caused by swelling because the samples are baked between measurements to remove solvent. The fact that UV irradiation appears to be more efficient than X-rays in this regard (Fig. 22) may result from the higher energy of the radiation in question (see Fig. 19) or more efficient absorption of UV energy by the ester group. It is unclear why the electron beam apparently causes more overgrowth than the more massive proton, but it is tempting to assume that a larger portion of the dose may be efficient at causing bond cleavage for electrons than for protons. In both cases, however, it is apparent that the amount of overgrowth increases with the incident dose.

A further interesting observation [11] was made based on the data in Fig. 24 where solubility is plotted against time for two electron beam doses and several solvents. The three steep lines at the bottom left of the figure are for unirradiated PMMA with three different solvents. After irradiation and treatment with acrylic acid, samples of modified PMMA were treated with the indicated solvents and the dissolution rates were monitored. At the higher dose (10^{-6} C/cm^2) all solvents are essentially equally poor but at the lower dose (10^{-7} C/cm^2) the more aggressive solvents give non-linear development patterns. This result was interpreted as reflecting a gradient of acrylic acid incorporation through the thickness of the film causing more extensive modification near the bottom of the film than at the top. It was proposed that the gradient arose because oxygen could diffuse slowly through the film inactivating more radicals at the top than at the bottom of the film. This interpretation is probably incorrect because it is in conflict with the known diffusion rate of O_2 in PMMA[12] and with recently acquired data on concentration profiles of chloroacrylic acid (vide infra). An alternative explanation which may be correct is that more modification occurs in the upper portions of the film

and when solvent development takes place the less modified bottom portions of the film dissolve first, allowing the less soluble upper layers to settle into the developing features.

The observation of vertical growth suggests that growth in the lateral dimension might also be possible with a resulting impact on image fidelity. The approach to the answer to this question is outlined in Fig. 25. A pattern of equally sized lines (dimension a) and spaces (dimension b) were generated using UV in the in situ process. If replication fidelity is high the ratio of the measured (SEM) line widths to spaces should be equal to one. It can be seen by an examination of the data presented in Fig. 26 that numbers larger than one are obtained at some doses indicating that lateral growth does occur. However, it can also be seen that this phenomenon can be controlled by appropriate adjustment of the dose. An apparent optimimum dose under the given operating conditions is about 20 mJ/cm^2 which yields faithfully replicated images.

PMMA has poor resistance to plasma and reactive ion etching so that it cannot be developed effectively by so-called dry methods. We examined acrylic acid-modified PMMA but found that it was still not sufficiently plasma resistant to cause an effective difference in dry etch rate between it and unirradiated PMMA. Poly(acrylic acid) contains many carboxylic acid groups which can easily exchange protons with positive ions (Na^+, K^+, Ca^{+2}, Mg^{+2}, Al^{+3}).[13,14] It is to be expected that incorporation of ions in this fashion should drastically improve the etch resistance of modified PMMA. This highly desirable result was achieved using the electronically inactive calcium ion.[15] The process termed "calcination" is outlined in Fig. 27. Films of acrylic acid-modified PMMA which had imbibed calcium ion by being soaked in a 20% aqueous calcium acetate solution at 60°C for specified times were exposed to an oxygen plasma and the results are shown in Fig. 28. The slopes of the lines for PMMA and modified (UV) PMMA are essentially the same, indicating no difference in etch rate, while the longer the modified films are soaked in the calcium ion solution, the more resistant to the plasma they become. If the radiation dose is increased then more modification should occur enabling more calcium ion to be incorporated and thereby enhance the etch resistance. Exactly this result is demonstrated in Fig. 29 for samples irradiated at increasing electron beam doses. If the films etched in

an oxygen plasma are subjected to reactive ion etching with fluoroform they are also found to be inert, within experimental error, Fig. 30, under conditions which etch silicon dioxide at a rate of 270 Å/min. A scanning electron micrograph of the pattern etched in Ca-AA-PMMA (20 mJ/cm^2, DUV, 1.5 μ line) by an oxygen plasma is shown in Fig. 31. It is readily seen that this approach confers sufficient contrast to generate images by dry etching. The RIE rate of of silicon dioxide is sufficiently fast compared to that of oxygen plasma-etched Ca-AA-PMMA that the image so generated should be directly transferable into the underlying silicon dioxide layer. An example of an image generated in this way is shown in Fig. 32. Careful examination of this micrograph reveals two layers, "oxidized-fluoridized" Ca-AA-PMMA atop SiO_2. Treatment of the resist residue with Caro's acid (H_2O_2-H_2SO_4) generates a pattern of 0.75 μ lines of silicon dixide, Fig. 33. Auger spectroscopic analysis of a film of Ca-AA-PMMA generated by DUV irradiation at 40mJ/cm^2 demonstrates the incorporation of calcium ion, Fig. 34. The changes engendered by exposure to oxygen and fluorine plasmas are evident in the Auger spectra shown in Fig. 35. The increase in oxygen content on plasma treatment is presumed to be the result of formation of involatile CaO. Similarly, incorporation of fluorine represents partial conversion of CaO to CaF_2, which is also involatile.

The elegant element profiling studies reported by Valenty et al.[16] for small molecules in polymer films led us to attempt to determine the distribution of modifying monomer chemically bound in our films by attaching chlorine to it and then analyzing by Auger electron spectroscopy(AES) and secondary ion mass spectrometry (SIMS). Our very preliminary results using AES and SIMS to this end are shown In Fig. 36 and 37, respectively. The traces shown in Fig 36 are, from top to bottom,for carbon, chlorine oxygen and silicon. It is clear that chlorine is present throughout the film. The apparent decrease in chlorine content near the surface of the film may reflect ejection of fragments of the polymer film during the sputtering process. In the SIMS profile shown in Fig. 37 the apparent chlorine content of the film decreases as the sputtering process erodes the film. The data obtained so far for both methods show that chlorine is present throughout the film but they differ with respect to the concentration gradient. Charging

effects and the possibility of scrambling of chlorine atoms under ion impact cloud the detailed interpretation of these data.

During our attempts to optimize process conditions, we determined that residual amounts of solvent could markedly affect the film thickness generated under the high dose (UV) conditions discussed above. When films of PMMA are spun from benzene solution and then baked for different times and temperatures the spectra shown in Fig. 38 are obtained. Traces 1 - 5 represent decreasing amounts of benzene remaining in the films if the baking process is not completed. Trace 6 is the spectrum of pure PMMA. If these films containing different amounts of benzene are photolyzed at a dose of 60 mJ/cm^2, the overgrowths generated vary with solvent content as shown in Fig. 39. At high concentrations the resulting film thicknesses are generally decreased compared to those observed in the absence of occluded solvent, while intermediate concentrations enhance the amount of film growth. It is tempting to conclude that these results are caused by photochemical quenching or sensitization effects, but such a conclusion awaits more detailed experimentation.

The model we have been using for the in situ modification process contains the assumption that acrylic acid somehow selectively penetrates the radiation damaged region. If that assumption is accurate, then we should be able to measure differences in the weight of absorbed acrylic acid and/or water before and after irradiation. Grant Willson of IBM was kind enough to provide us with the construction details for a quartz crystal microbalance used in his group to measure resist dissolution rates. The incorporation of this device into our reaction apparatus is shown in Fig. 40. Initial results obtained with this new apparatus using 2-propanol as a model penetrant are shown in Fig. 41. As hypothesized, increasing the irradiation dose enhances the amount of penetrant imbibed by the film. When this experiment is performed using pure water as the penetrant, essentially no difference in diffusion rate is detectable upon irradiation, even up to doses as high as 2 J/cm^2, Fig. 42. When aqueous acrylic acid is used as the permeating substance, hardly any effect on the amount of monomer absorbed is detectable except at doses much larger than those necessary to generate easily detectable solubility differences. We presume that the accelerating weight gain observed at the highest dose used in Fig. 43 reflects the enhanced hydrophilic

nature conferred on the film by incorporation of acrylic acid. At this time we can see no simple way to determine which portion of the weight gain is caused by absorption of water and which by absorption of monomer. Either the amount of acrylic acid absorbed at doses which permit image generation as shown above are within the range of experimental error (±4 μg) or their is no selectivity to the absorption of acrylic acid by irradiated PMMA. The observation of lateral image growth as reported above would seem to support this latter surmise. The only factor remaining which would confer the selectivity needed to account for the generation of images is that the concentration of reactive free radical centers is anisotropic over the surface of the film, being physically restricted to the radiation damaged regions below the glass transition temperature of PMMA. Thus, initiation occurs only in the damaged areas and propagation of growing chains occurs in all directions. After the initial radiation event no net increase in radical concentration can occur so that, eventually, polymer chain growth must cease because of radical termination processes. Given the observations made above that image fidelity is quite good under optimized conditions, it appears that the amount of chain growth beyond the irradiated areas is inconsequential.

This account should be considered as an interim report on our continuing efforts to elucidate the detailed nature of this intriguing process.

ACKNOWLEDGEMENT

The diligence of the students involved was the sine qua non of this effort. The technical support rendered by M. Bourgeois, D. King, N. King, D. Pulver and the late D. Winterhalter, all of the Center for Integrated Electronics, represents the base upon which our efforts are built. Many extramural colleagues were magnanimous with their knowledge, equipment and expertise. Among these are Drs. P. Hood, W. Moreau, J. Silverman and C. G. Willson of IBM, Dr. D. Skelly of G. E. and Dr. J. Randall of MIT's Lincoln Lab. The SIMS measurements were performed by Bela Vastag under the aegis of Dr. R. Thomas at Griffis Air Force Base, R. A. D. C., Rome, NY. The lamp used in the UV irradiations was graciously provided by J. Bachur of the Hybrid Technology Group. Generous financial support

of this program up to this point has been provided by the IBM Corporation and the Semiconductor Research Corporation.

REFERENCES

[1] Wayne M. Moreau, Optical Engineering, **22**, 181 (1983).

[2] C. G. Willson, in *Introduction to Microlithography*, L. F. Thompson, C. G. Willson and M. J. Bowden eds., ACS Symposium Series #219, American Chemical Society, Washington, DC, 1983.

[3] A. C. Ouano, Polym. Eng. Sci., **18**, 306 (1978).

[4] D. Follett, K. Weiss, J. A. Moore, A. J. Steckl and W.-T. Liu, Abstracts of the Electrochemical Society Meeting, Detroit, MI, 1982.

[5] A. Gazard, C. Duchense, J. C. Dubois and A. Chapiro, Polym. Eng. Sci., **20**, 1069 (1980).

[6] R. M. Tarro, J. T. Warden, J. C. Corelli, J. A. Moore, A. J. Steckl and S. Kumar, *Microcircuit Engineering 84*, A. Heuberger and H. Beneking, eds., Academic Press. London, 1985, p. 538.

[7] H. Hiraoka, IBM J. Res. Develop., March 1977, 121.

[8] W.-T. Liu, M. Bourgeois, J. A. Moore, J. C. Corelli and A. J. Steckl, J. Electrochem. Soc., **82-2**, 331 (1983).

[9] W.-T. Liu, J. C. Corelli, A. J. Steckl, J. A. Moore and J. Silverman, Appl. Phys. Lett., **44**, 973 (1984).

[10] J. A. Moore, J. C. Corelli,A. J. Steckl, J. T. Warden, W.-T. Liu, R. Tarro and J. N. Randall, Polym. Prepr., **25**, 105 (1984).

[11] S. Y. Kim, J. Choi, D. Pulver, J. A. Moore, J. C. Corelli and A. J. Steckl, J. Vac. Sci. Technol., **B4**, 403 (1986).

[12] B. Rånby and J. F. Rabek, in *Photodegradation, Photo-oxidation and Photostabilization of Polymers*, John wiley and Sons, New York, 1975, p. 105.

[13] C. C. Anderson, and F. Rodriguez, J. Vac. Sci. Technol., **B3**, 347 (1985).

[14] J. Economy, J. R. Lyerla and L. A. Pedersen, U. S. Patent No. 4 289 573 (Sept. 15, 1981).

[15] J. O. Choi, S. Y. Kim, J. A. Moore, J. C. Corelli and A. J. Steckl, J. Vac. Sci. Technol., **B5**, 382 (1987).

[16] S. J. Valenty, J. J. Chera, D. R. Olson, K. K. Webb, G. A. Smith and W. Katz, J. Am. Chem. Soc., **106**, 6155 (1984).

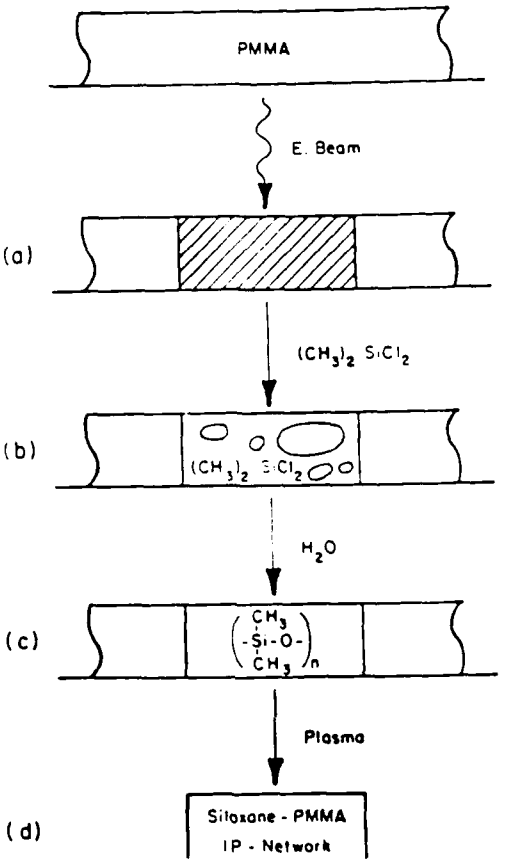

Fig.1 Silylation Process Schematic

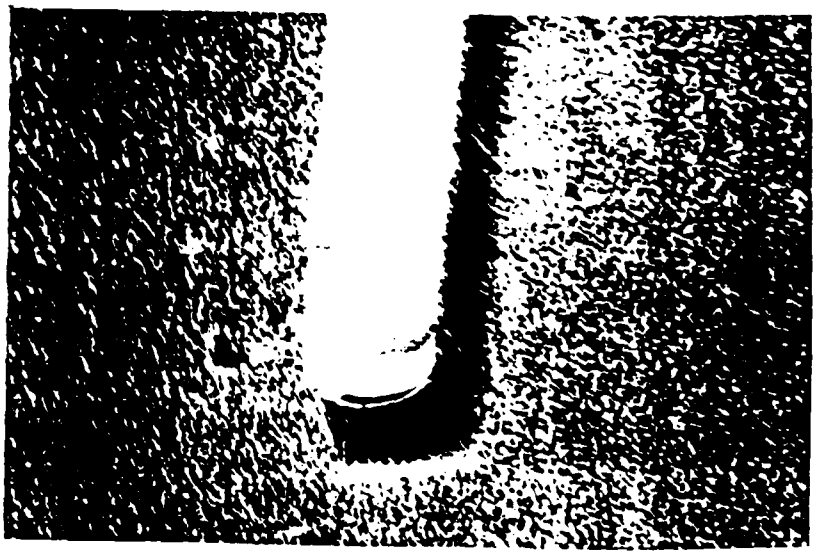

Fig.2 Siloxane-PMMA 2μ line

- POSITIVE TONE LITHOGRAPHY
  - CHAIN DEGRADATION TO "DEAD" FRAGMENTS
  - ENHANCED SOLUBILITY OF SMALLER FRAGMENTS
- IN-SITU MODIFICATION
  - CHAIN DEGRADATION
  - CHEMICAL TRAPPING OF REACTIVE CENTERS
  - NEGATIVE TONE BY SOLUBILITY ALTERATION

Fig.3 Process Comparison

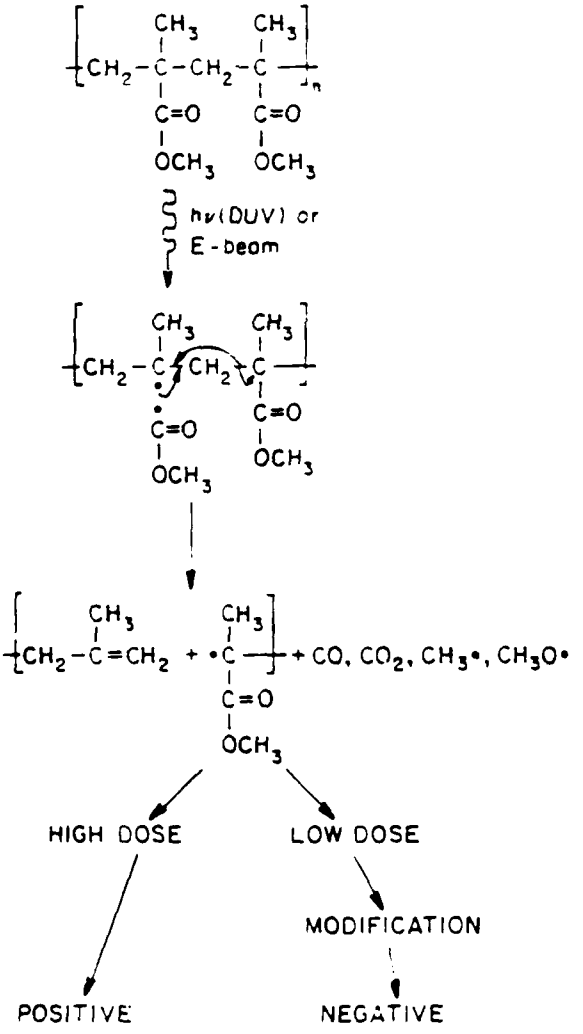

Fig.4 PMMA Radiolysis

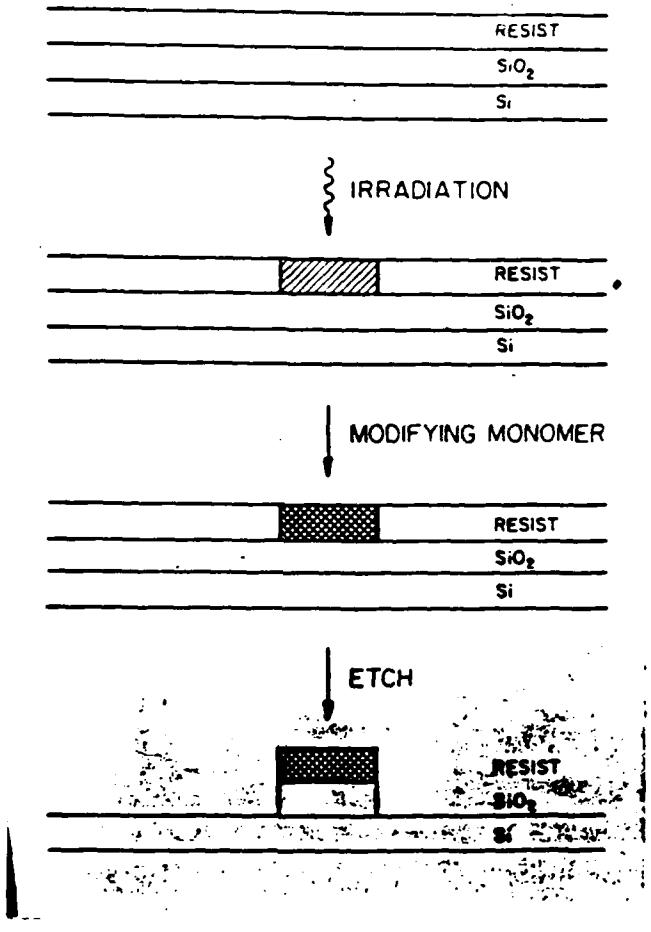

Fig.5 In Situ Modification

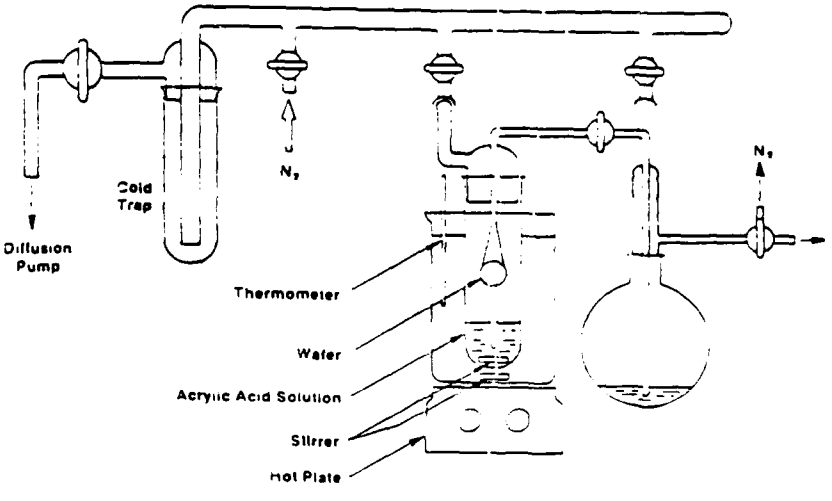

Fig.6 Reaction Apparatus

PMMA IRRADIATION

CHEMICAL TREATMENT
* ACRYLIC ACID VAPOR
* BASE PRESSURE = 10-6 TORR
* 60 °C
* 10 - 40 MIN.

POSTBAKE
* 120°C, 15 MIN.

DEVELOPMENT
* TOLUENE
* 40°C, 5-10 MIN.

Fig.7 Basic Process

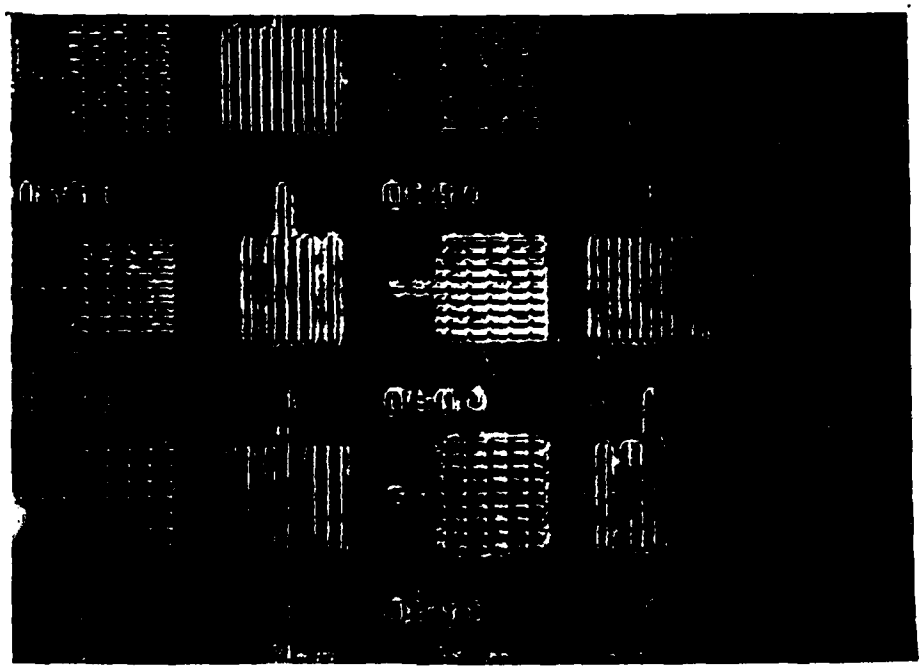

Fig.8 Undeveloped Image

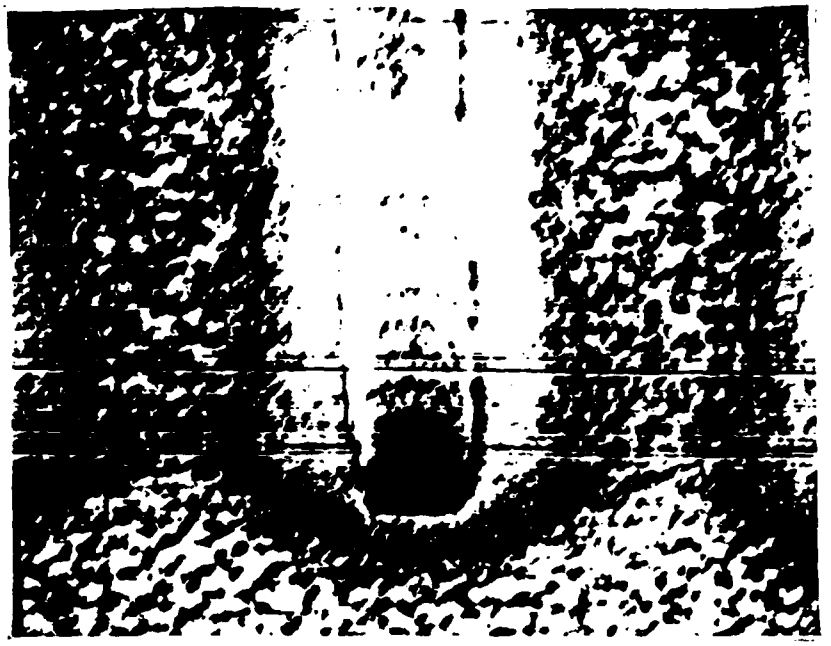

Fig.9 E-Beam 2μ, $10^{-8}C/cm^2$

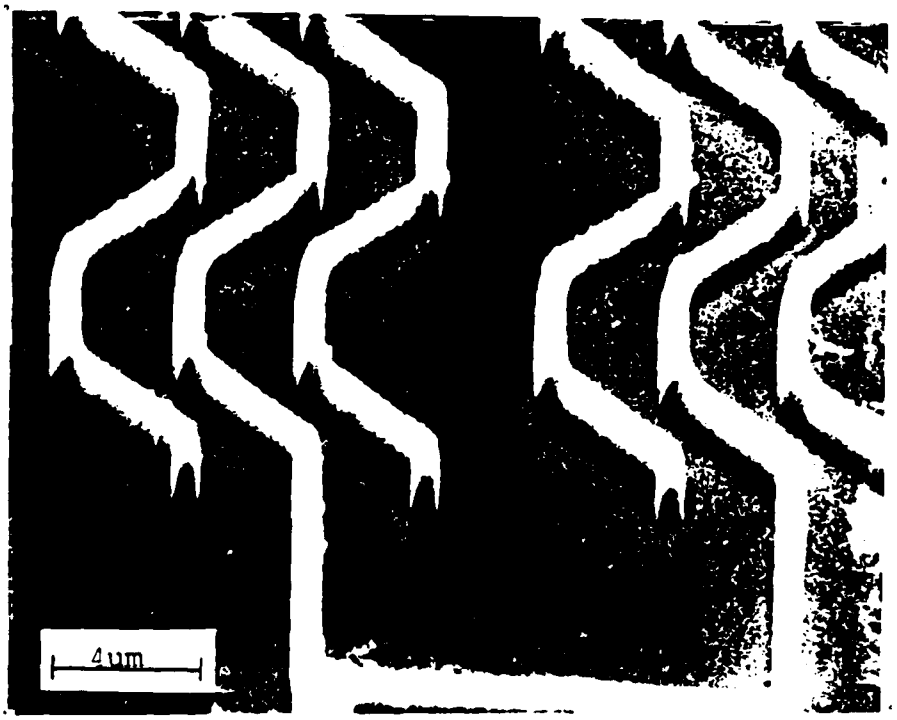

Fig.10 X-Ray (+), 1 J/cm^2

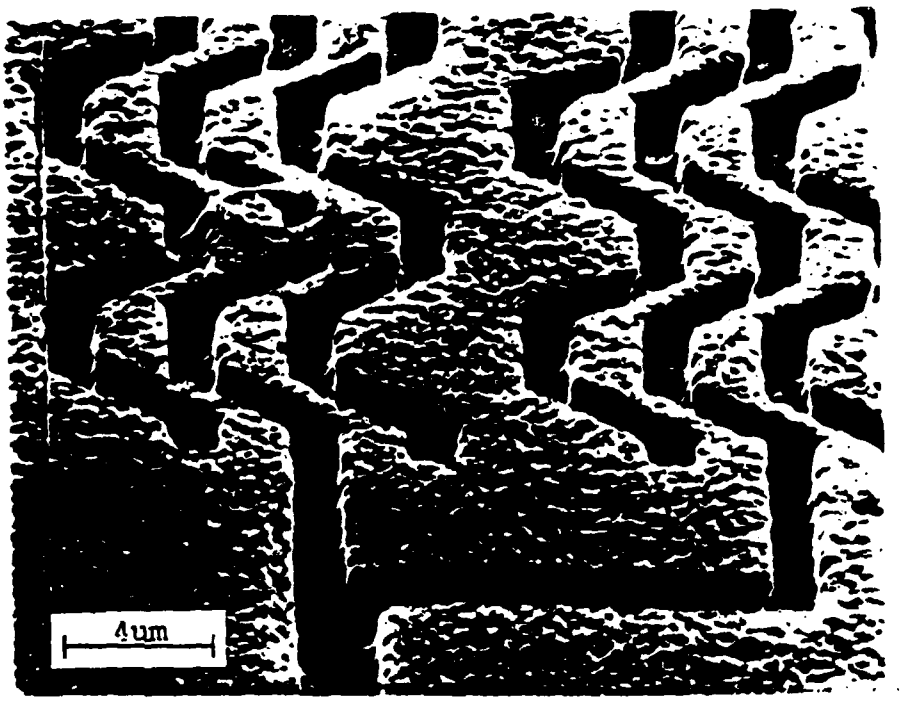

Fig.11 X-Ray (-), 1 mJ/cm^2

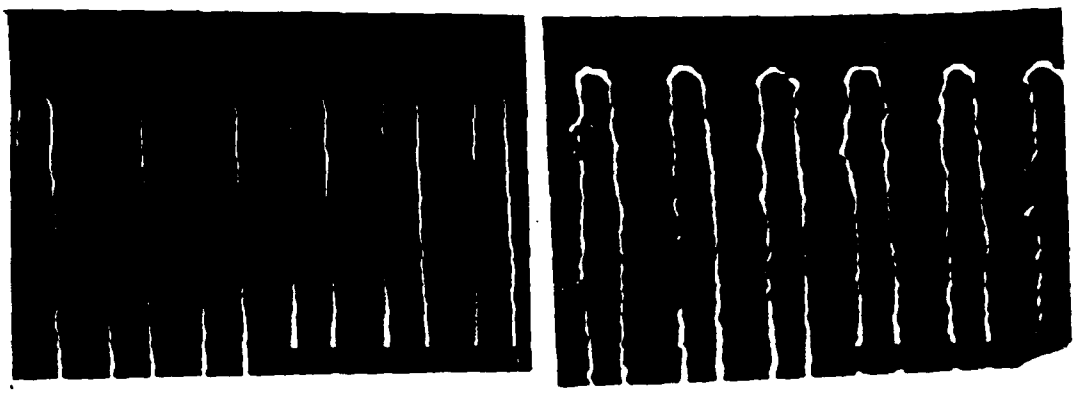

Fig.12 X-Ray Image Fidelity
Left (+), Right (-)

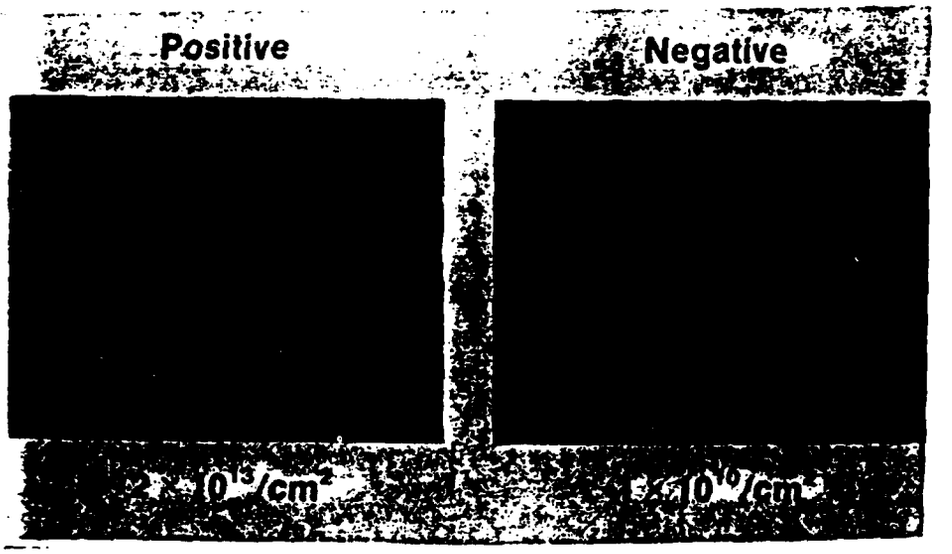

Fig.13 H^+ Beam Comparison

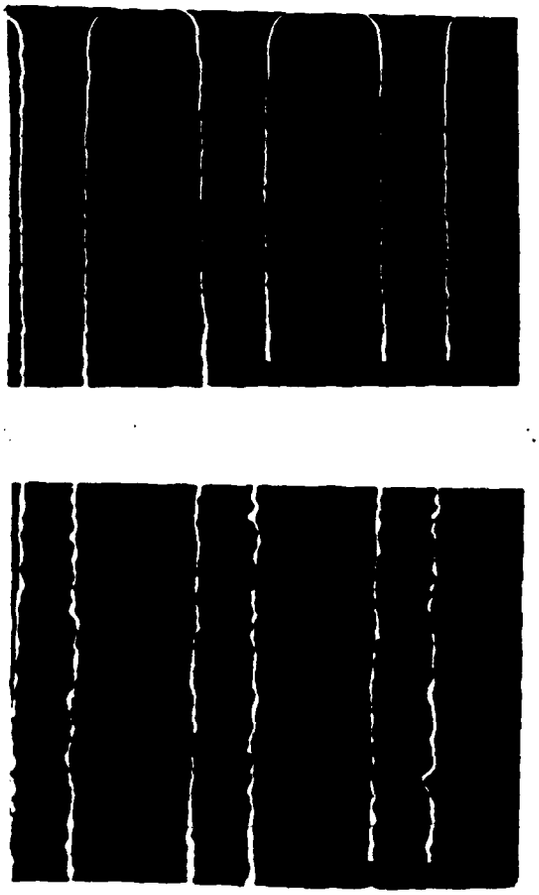

Fig.14 H^+ Image Fidelity
Upper (+), Lower (-)

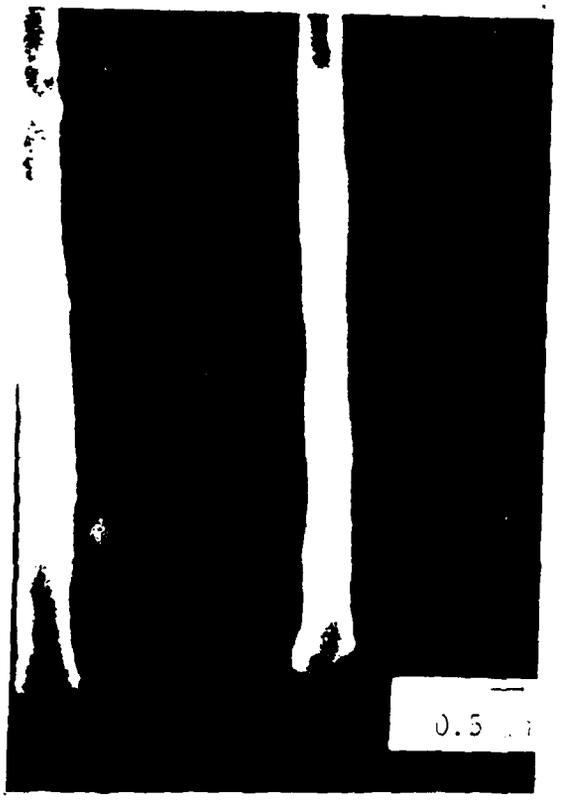

Fig.15 Sub 0.5μ Line, H^+ Beam

Fig.16 Modification of H^+ Track

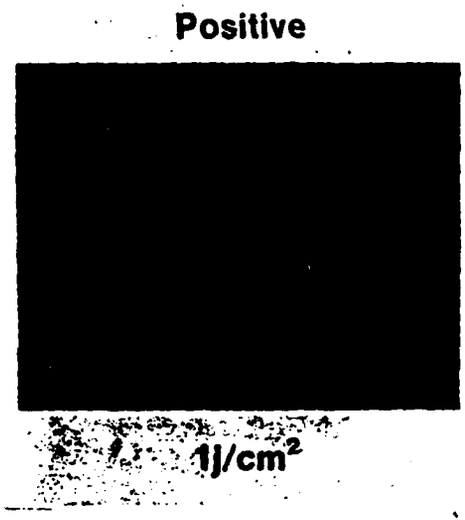

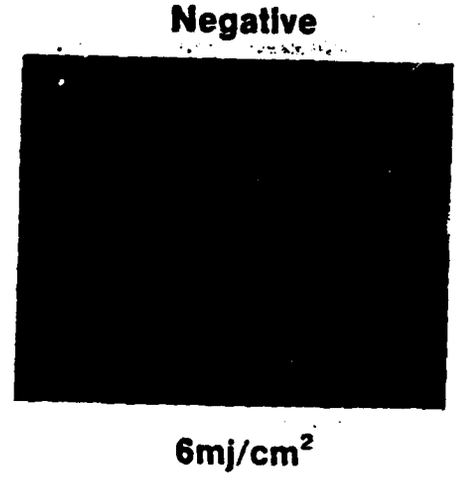

Fig.17 UV Comparison
Upper (+), Lower (-)

Fig18 Sub 1μ Line, UV

	H^+ (100 KeV)	X-Ray (0.5-1.5 KeV)	E-Beam (20 KeV)	UV (5.3eV)
Normal Exposure Dose	10^{13} Ions/cm^2	1 J/cm^2	2×10^{-5} C/cm^2	1 J/cm^2
Lowest Effective Modifying Dose	10^{9} Ions/cm^2	10^{-3} J/cm^2	10^{-8} C/cm^2	2.5×10^{-3} J/cm^2
Particle Flux	10^{9} Ions/cm^2	6×10^{13} Photons/cm^2	6×10^{11} e$^-$/cm^2	3×10^{15} Photons/cm^2
Incident Energy	1.5×10^{-5} J/cm^2	10^{-3} J/cm^2	2×10^{-4} J/cm^2	2.5×10^{-3} J/cm^2
Image Gain	10^4	10^3	2×10^3	4×10^2

Fig.19 Comparison of Effective Doses

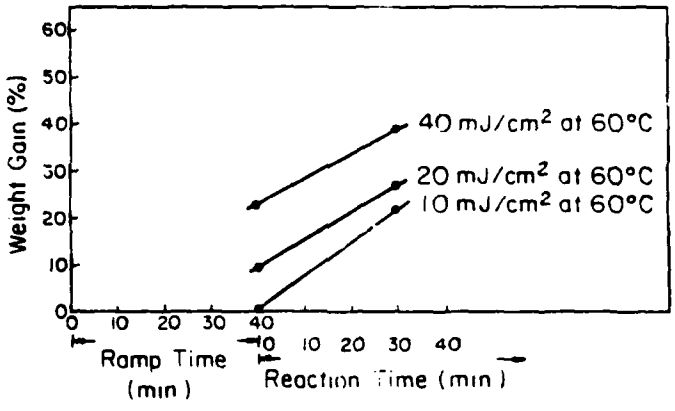

Fig.20 Wt. Gain vs. UV Dose

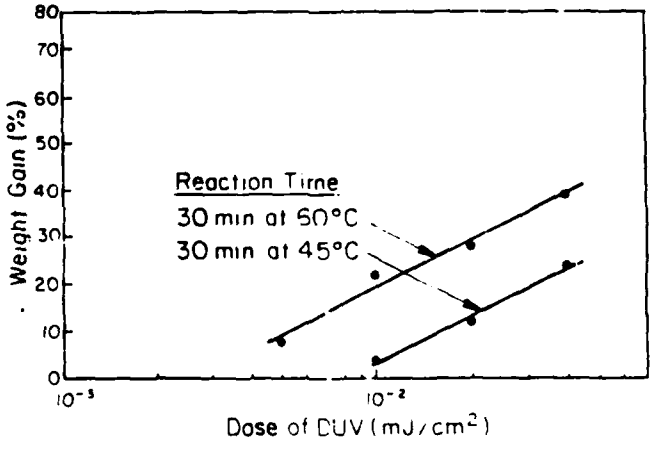

Fig.21 Wt. Gain vs. Dose. Effect of Temperature

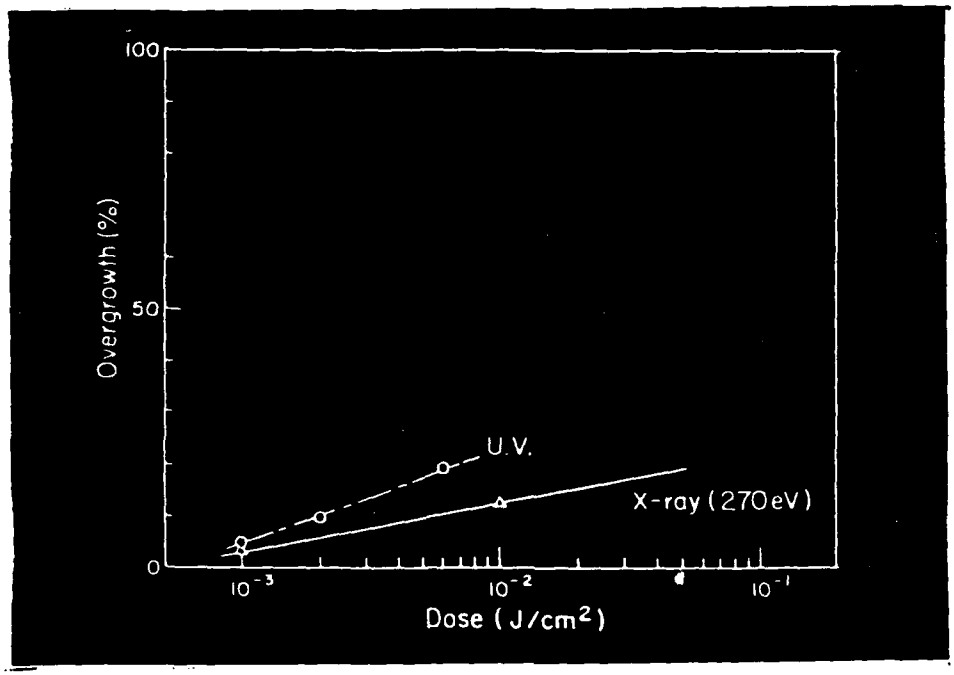

Fig.22 Overgrowth vs. Dose
(UV and X-Ray)

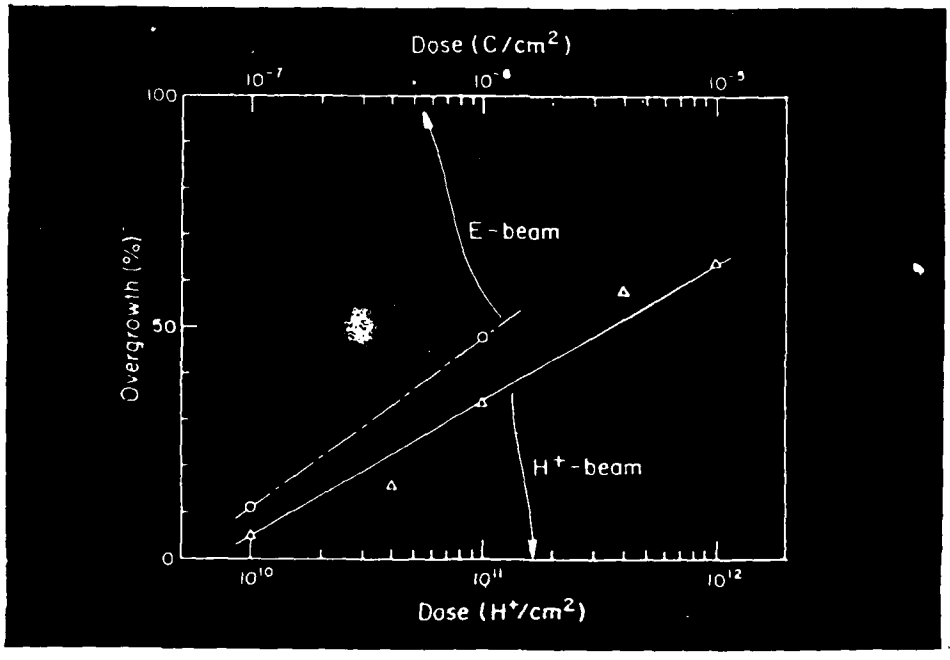

Fig.23 Overgrowth vs. Dose
(H^+ and E-Beam)

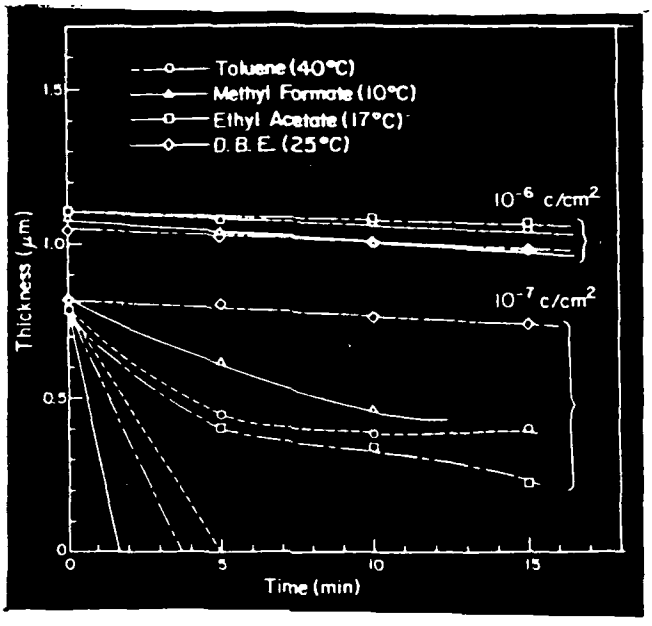

Fig.24 Solvent Development

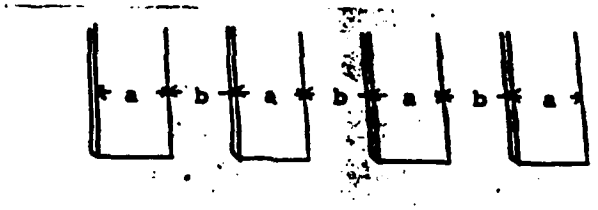

$$\text{Ratio} = \frac{\text{average a}}{\text{average b}}$$

Fig.25 Image Fidelity Test Pattern

Image / UV Exposure Dose	Ratio of b/a	Mask Region 1	Mask Region 2
Positive Image	1000 mJ/cm^2	1.33	1.19
Negative Image	4 mJ/cm^2	0.31	0.47
	16 mJ/cm^2	Run 1 0.72	0.94
		Run 2 0.98	1.04
	30 mJ/cm^2	1.27	1.43

Fig.26 Image Fidelity Data

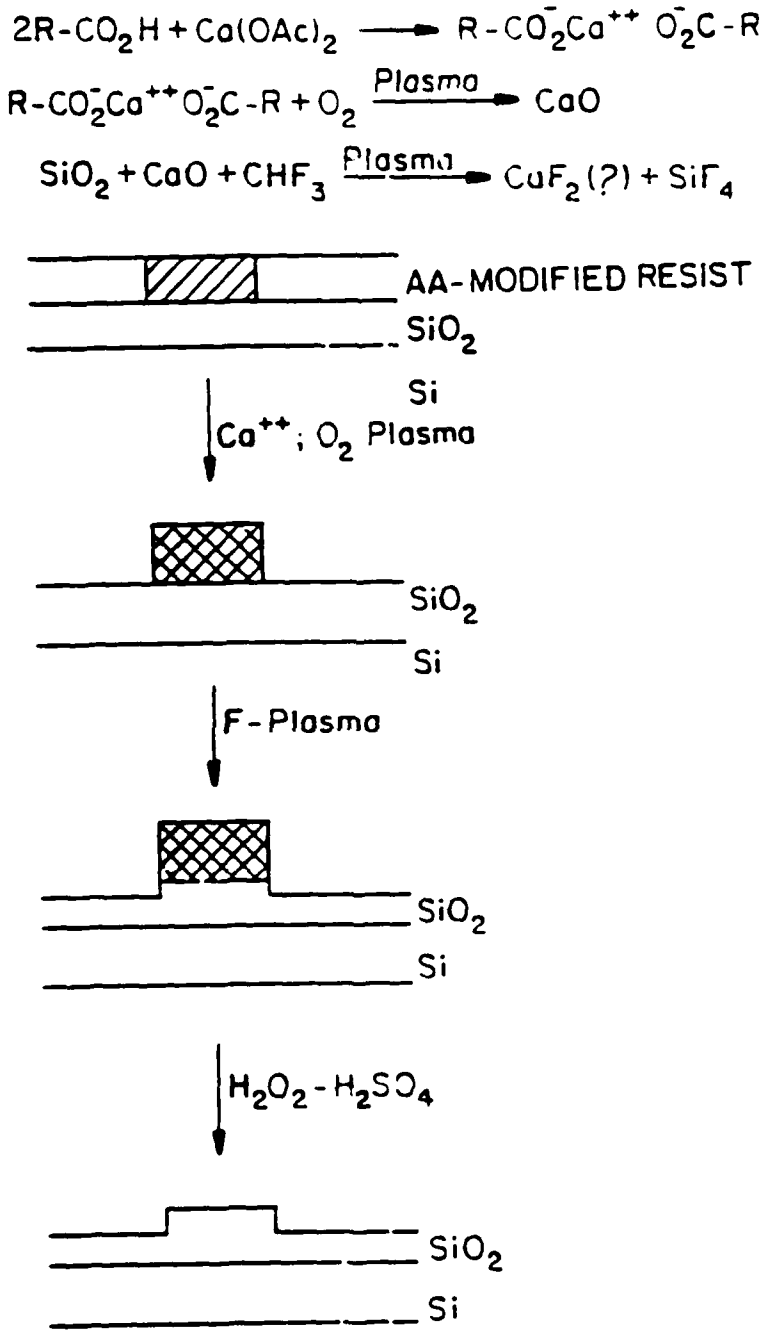

Fig.27 Calcination Process

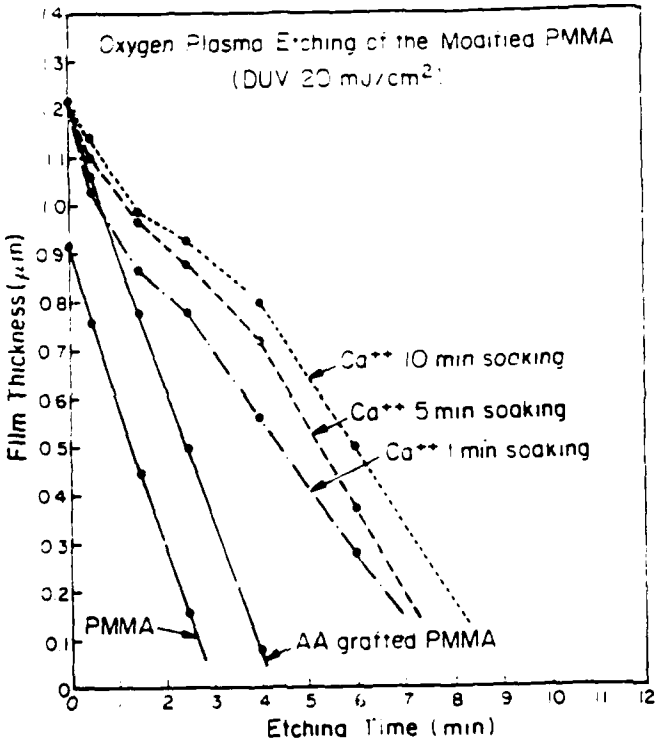

Fig.28 O_2 Plasma Etch vs. Soak Time

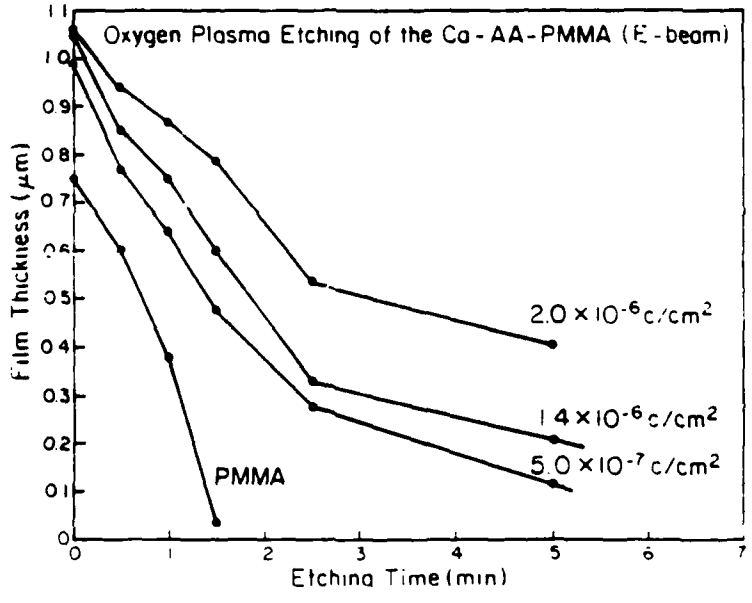

Fig.29 O_2 Plasma Etch vs. Dose

Material	O_2-Plasma*	CHF_3 RIE**
PMMA	3040 A°/min	330 A°/min
AA-PMMA (20 mJ/cm^2)	2880 A°/min	110 A°/min
Ca-AA-PMMA (20 mJ/cm^2)	1160 A°/min	10 A°/min (after O_2-Plasma)
SiO_2	0 A°/min	270 A°/min

* 110 mTorr, 255 Watt, 2.5 min

** 34 mTorr, 300 Watt, 10 min

Fig.30 Dry Etch Rates

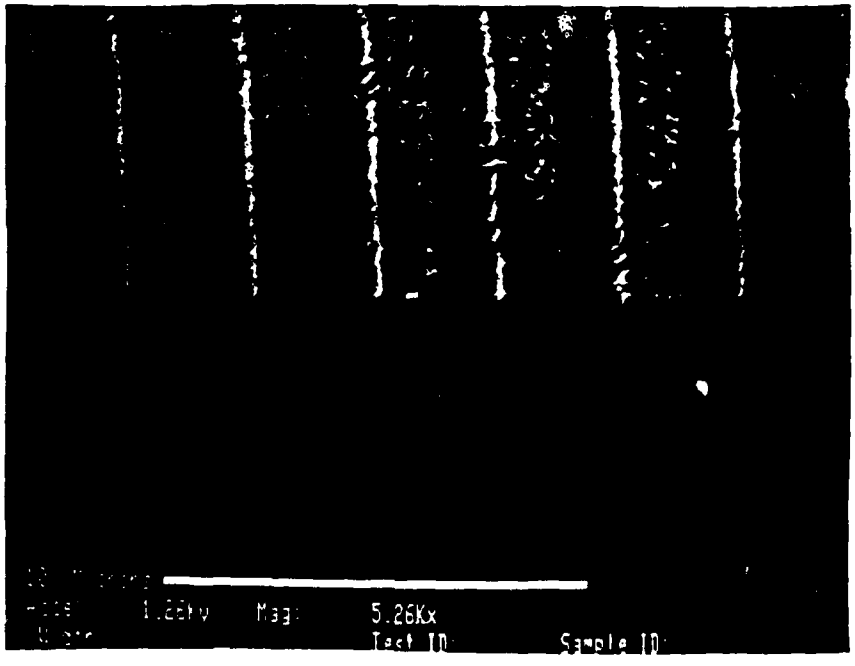

Fig.31 O2-Plasma Etched Images

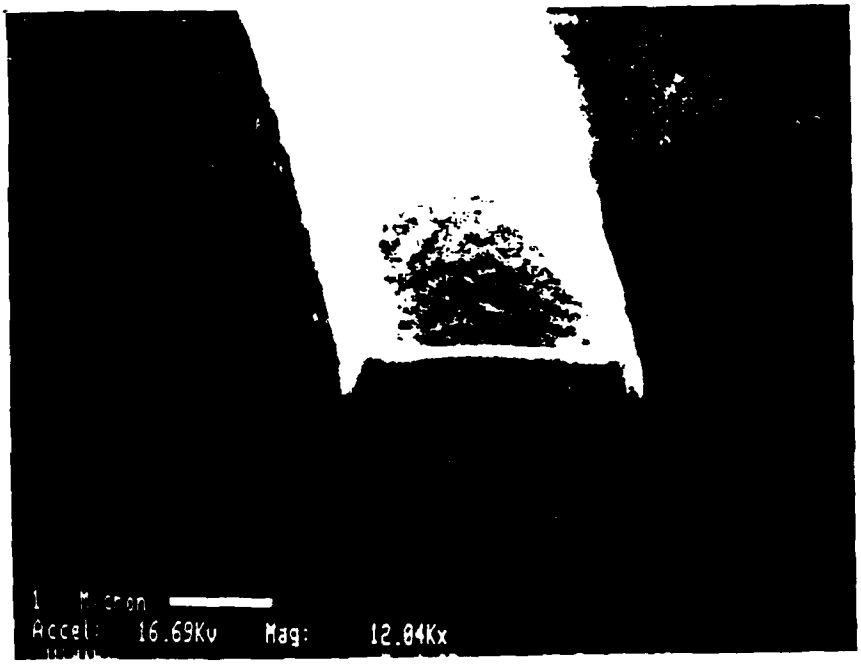

Fig.32 Previous Image After CHF_3 RIE

Fig.33 Previous Image After Stripping

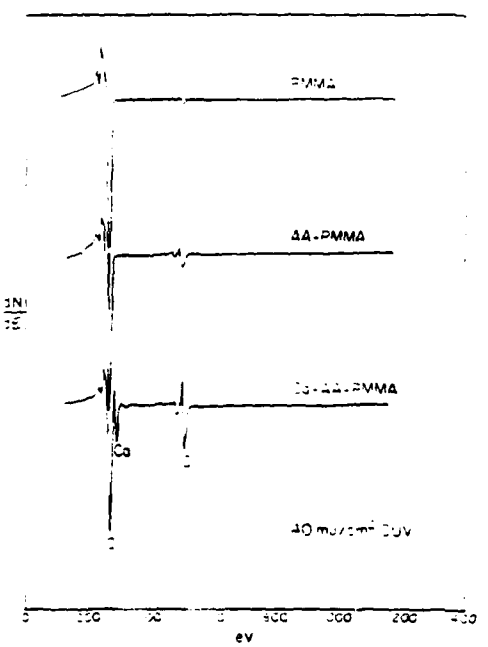

Fig.34 Auger Spectrum of Calcinated PMMA

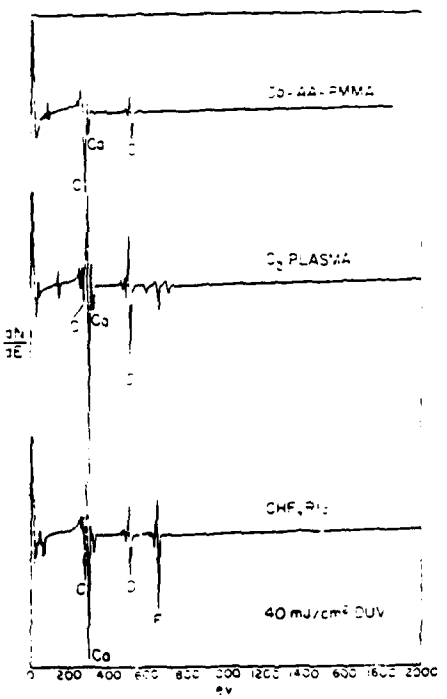

Fig.35 Auger Spectrum of Calcinated PMMA After Etching

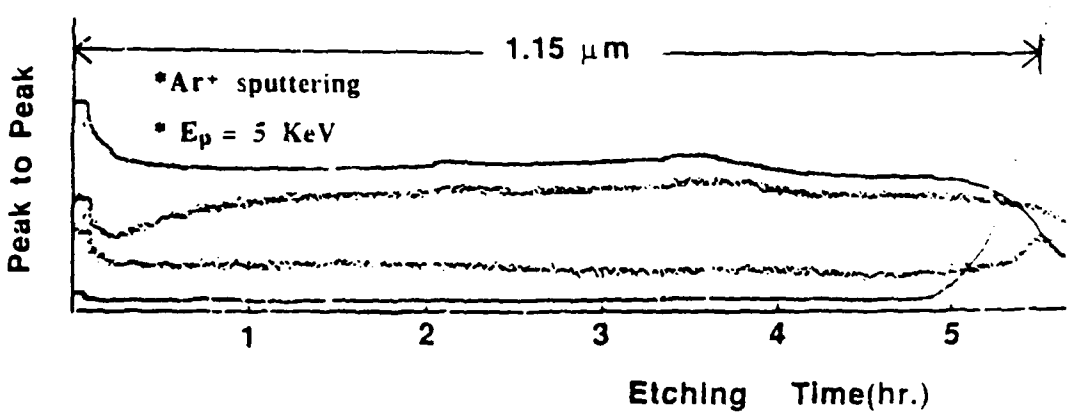

Fig.36 Penetration Profile (Auger)

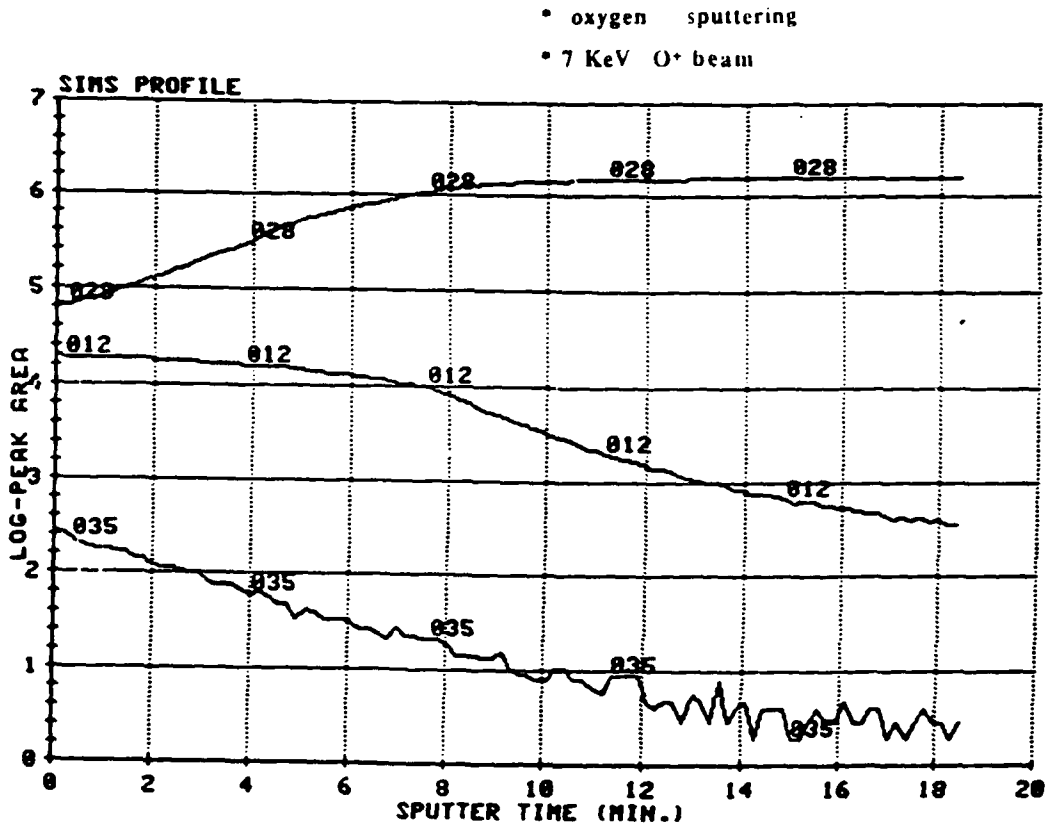

Fig.37 Penetration Profile
(SIMS)

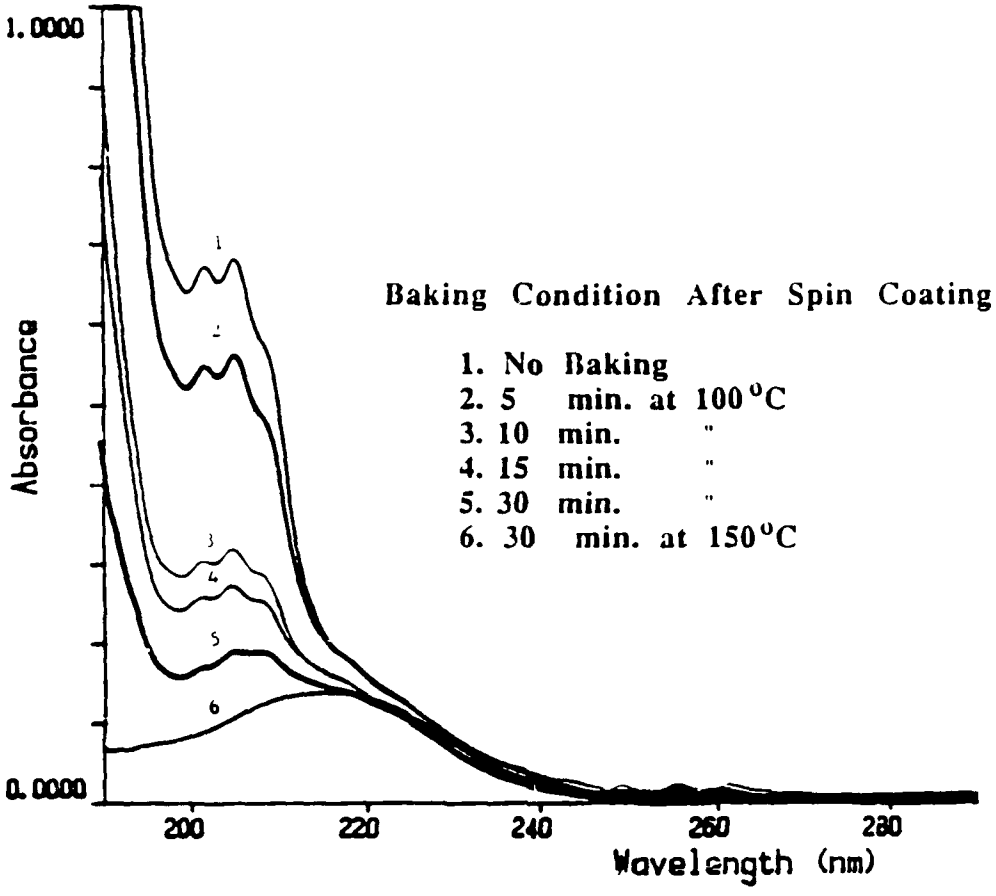

Fig.38 UV Spectrum of Residual Solvent

S / 100M \ Sensitizer(S)	Benzene	Toluene	Chlorobenzene
20	N.D.	N.D.	11 %
8	18 %	8 %	41 %
3	46 %	27 %	N.D.
0	24 %	20 %	20 %

N.D. : Not Determmed

Fig.39 Effect of Trapped Solvent On Overgrowth (60 mJ/cm^2)

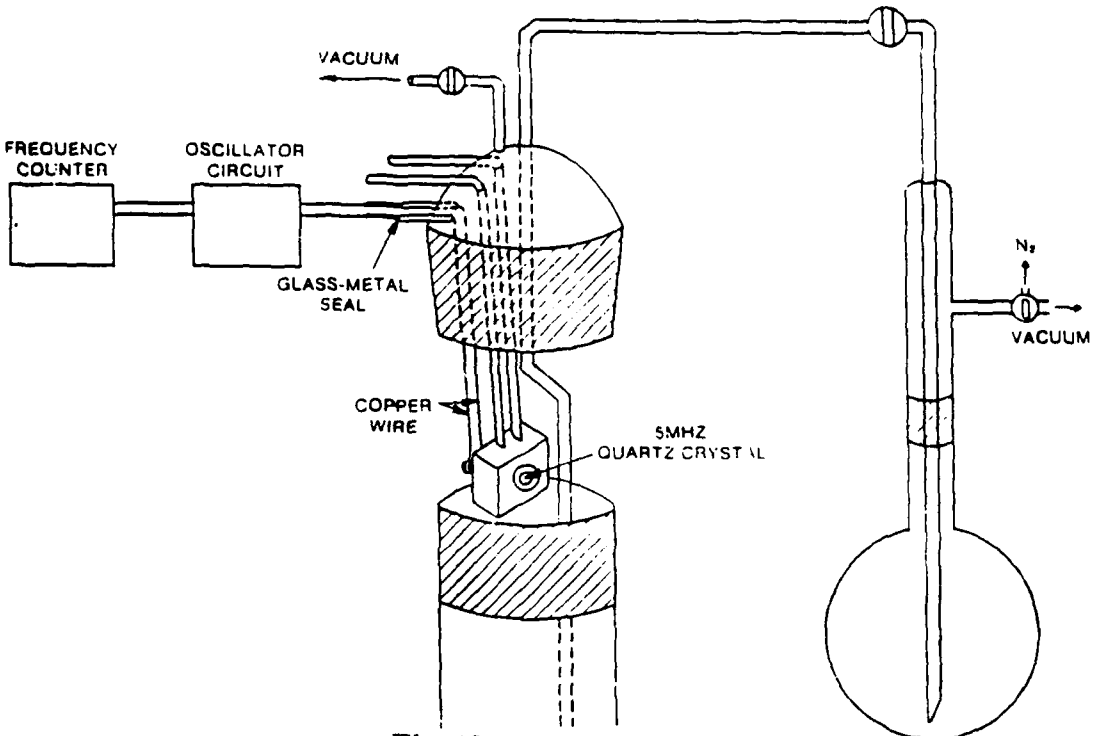

Fig.40 Modification of Appparatus

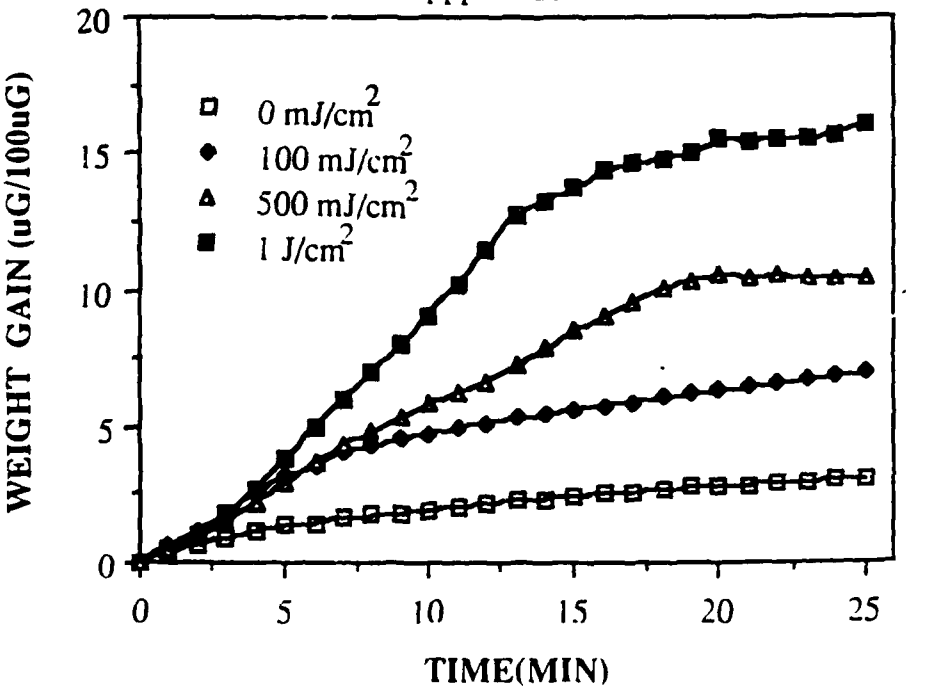

Fig.41 Wt. Gain of 2-Propanol vs. Dose

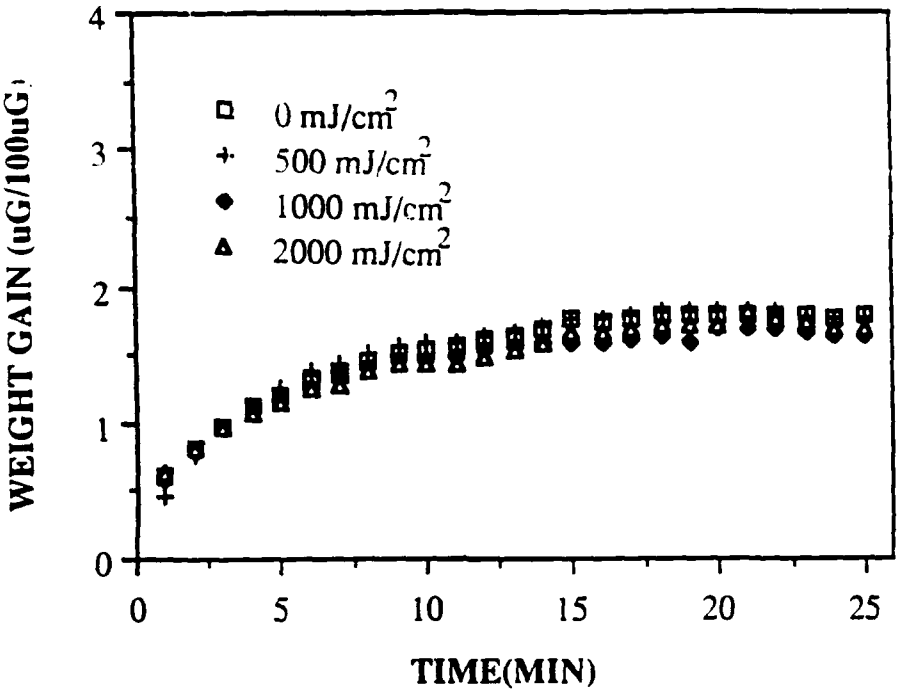

Fig.42 Wt. Gain Of Water vs. Dose

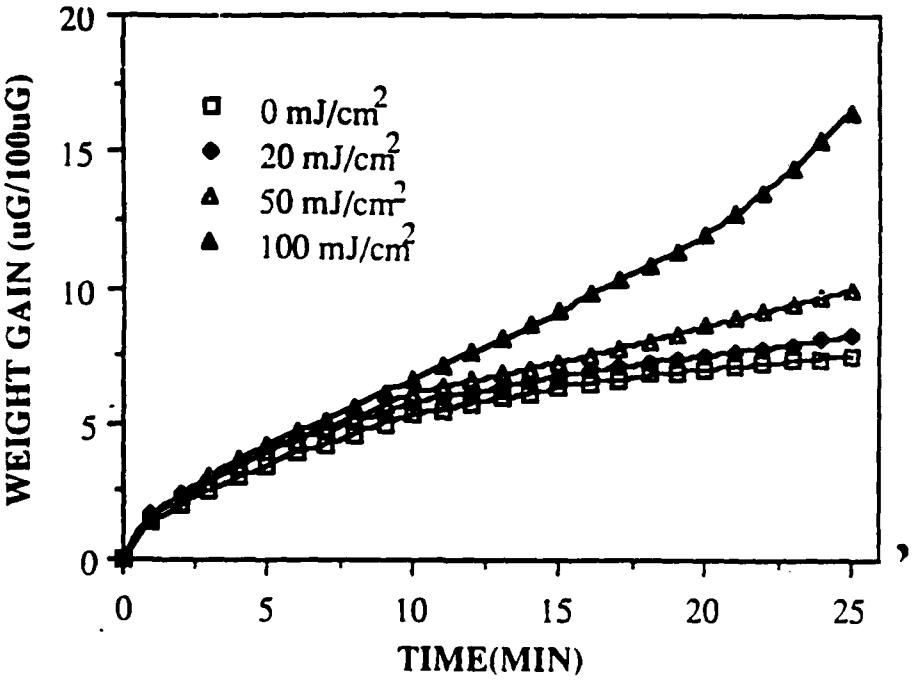

Fig.43 Wt. Gain of Aq. Acrylic Acid vs. Dose